Exp Brain Res (1998) 119:375–390

RESEARCH ARTICLE

Achim Rumberger · Matthias Schmidt
Horst Lohmann · Klaus-Peter Hoffmann

Correlation of electrophysiology, morphology, and functions in corticotectal and corticopretectal projection neurons in rat visual cortex

Received: 22 November 1996 / Accepted: 8 October 1997

Abstract In most mammals the superior colliculus (SC) and the pretectal nucleus of the optic tract (NOT) receive direct input from the ipsilateral visual cortex via projection neurons from infragranular layer V. We examined whether these projection neurons belong to different populations and, if so, whether it is possible to correlate the electrophysiological features with the suggested function of these neurons. Projection cells were retrogradely labeled in vivo by rhodamine-coupled latex beads or fast blue injections into the SC or the NOT 2–5 days prior to the electrophysiological experiment. Intracellular recordings of prelabeled neurons were made from standard slice preparations and cells were filled with biocytin in order to reveal their morphology. Both cell populations consist of layer V pyramids with long apical dendrites that form terminal tufts in layer I. In electrophysiological terms, 12 of the corticotectal cells could be classified as intrinsically bursting (IB), while two neurons showed a doublet firing characteristic and one neuron was classified as regular-spiking (RS). Intracortical microstimulation of cortical layer II/III revealed that SC-projecting neurons responded optimally to stimulation sites up to a distance of 1000 μm from the recorded cell. The morphological features of the SC-projecting cells reveal an apical dendritic tuft in layer I with a lateral extension of 300 μm, a mean spine density of 65 spines per 40 μm on the apical dendrites located in layer II/III, and a bouton density of 13 boutons per 100 μm on the intracortical axons. Sixteen NOT-projecting neurons exhibited an IB and five cells an RS characteristic. Intracortical microstimulation of cortical layer II/III showed that NOT-projecting neurons responded optimally to stimulation sites up to a distance of 1500 μm. Their morphological features consist of an apical dendritic tuft with a lateral extension of 500 μm, a mean spine density of 25 spines per 40 μm on the apical dendrites located in layer II/III, and a bouton density of 6 boutons per 100 μm on the intracortical axons. When the passive membrane parameters, responses to intracortical microstimulation in layer V, the extension of the basal dendritic field, and spine densities in layers I or V were compared between SC- and NOT-projecting cells, no differences were revealed. Differences were only consistently found in the supragranular layers, either for morphological parameters or for intracortical microstimulation. The results suggest that NOT-projecting and SC-projecting neurons, although biophysically similar, could integrate and transmit different spatial aspects of cortical visual information to their target structures.

Key words Visual cortex · Superior colliculus · Nucleus of the optic tract · Electrophysiology · Morphology · Rat

A. Rumberger[1] · M. Schmidt · H. Lohmann[2] · K.-P. Hoffmann (✉)
Ruhr-Universität Bochum,
Department of General Zoology and Neurobiology,
D-44780 Bochum, Germany
Fax: +49-234-7094-185

Present addresses:
[1]Neurocenter Freiburg, Breisacherstr. 64, D-79106 Freiburg, Germany
[2]Lohmann Neuropharmacological Consulting,
Technologiezentrum Ruhr, Universitätsstr. 142, D-44799 Bochum, Germany

Introduction

Neurons in the superficial layers of the rat's superior colliculus (SC) possess restricted visual receptive fields and are optimally activated by small moving objects. In contrast, cells in the pretectal nucleus of the optic tract (NOT) have large, almost global receptive fields, and many of them show a clear directional preference for temporal to nasal movements when stimulated through the contralateral eye by large area patterns. Functionally, these differences in response properties may be related to the different tasks in visuomotor behavior mediated by these structures. The deep layers of the SC are assumed to coordinate movements of the eyes, head, and body during the execution of orienting reflexes to specific targets in space (Huerta and Harting 1984). In contrast, the nuclei of the pretectal complex mediate nontopographic reflexes such as pupil constriction or gaze stabilization and optokinetic

nystagmus (Schoppmann and Hoffmann 1979; Hoffmann and Distler 1986; Hoffmann 1989). Both the SC and the NOT receive, in addition to direct retinal input (Hoffmann and Schoppmann 1975; Linden and Perry 1983; Hoffmann and Stone 1985; Zhang and Hoffmann 1993), input from the ipsilateral visual cortex (Sefton et al. 1981; Harting et al. 1992; Schmidt et al. 1993). In order to fulfill their different tasks correctly, the subcortical structures need specific and probably different information from their input structures. Indeed the retinotectal and retinopretectal retinal ganglion cells most probably form nonidentical subpopulations (Hoffmann 1973; Hoffmann and Stone 1985). The corticofugal neurons projecting to the SC and NOT in cat may belong to different populations of layer V pyramidal cells, as suggested by Mader (1987). Concerning this question, so far only corticotectal neurons have been studied with regard to their morphological and electrophysiological parameters (Schofield et al. 1987; Hallman et al. 1988; Hübener and Bolz 1988; Wang and McCormick 1993; Tseng and Prince 1993; Kasper et al. 1994). These authors of these studies were able to demonstrate that all the corticotectal neurons possess an apical dendrite that reaches layer I and arborizes there in a tuft. Furthermore, they were able to demonstrate that corticotectal neurons can be classified as intrinsic bursting (IB) or as doublet-firing neurons.

In a more general approach, Chagnac-Amitai et al. (1990) and Larkman and Mason (1990) suggested an electrophysiological-morphological correlation in that all large layer V neurons could be characterized as IB, while the small layer V neurons should be classified as regular-spiking (RS) in their response pattern. No finer structure-function correlations have been noted, possibly because the populations of projection neurons studied were themselves very heterogeneous. Even a general correlation was questioned by Lohmann (1994), who found that neurons with an apical dendrite that reaches and arborizes in layer I in a tuft can also project to other cortical targets via the corpus callosum. Morphological parameters most frequently used to establish a structure-function correlation, such as the soma area (Hübener et al. 1990) or numbers of dendrites (Hallman et al. 1988) did not lead to a proper differentiation. No such investigation has yet been carried out for corticopretectal neurons.

We chose a slightly different strategy in our study. Neurons in the SC probably need information with a higher spatial resolution that corresponds to input from small parts of the visual field in order to achieve saccade generation and other orienting behavior, whereas pretectal neurons should receive movement information from large parts of the visual field in order to subserve the optokinetic reflex. The fact that neurons in the pretectal nucleus of the optic tract (NOT) of the rat do indeed receive direct information from the ipsilateral visual cortex was demonstrated in a study by Schmidt et al. (1993). If there are separate populations of projection cells to the SC and NOT, one would probably expect to find morphological differences between the two populations in the extension of their basal and apical dendritic trees and possibly in the number of spines. These parameters represent the ability of the neurons to collect and weigh information from the surrounding neuronal cortical network. Moreover, the intracortical axonal arborization representing the ability of the neurons to transmit information to the surrounding cortical network could be different.

Some of this work has been published in abstract form (Rumberger et al. 1994, 1995).

Materials and methods

Tracer injection

Rhodamine-labeled latex microspheres (RLMs; Lumafluor, USA) and fast blue (FB; Dr. Illing, Germany) were chosen as retrograde tracers (Katz et al. 1984; Tseng and Prince 1993). Long-Evans hooded rats were each anesthetized with 30 mg ketamine (Parke-Davis) plus 0.05 ml xylazine (Rompun; Bayer) on postnatal days 60–70. Penetrations were performed at 45° angles through the contralateral cortex to avoid damage or contamination to the neocortex, from which slices were to be taken later. The SC was first localized by means of stereotaxic coordinates (bregma –6.8 mm, lateral 2 mm). The exact localization was determined by extracellular single-unit recordings of the visual response properties. FB (2% FB, diluted in 2% DMSO) was pressure-injected unilaterally into one SC through a glass micropipette (tip diameter 30 µm) attached to a Hamilton syringe. Two injections (each of 0.15 µl volume) were given. The NOT was localized in the same way (bregma –5.3 mm, lateral 2.5 mm), except that the extracellular recordings were performed through the injection pipette. RLMs 0.2 µl (diluted 1:1 in 0.9% NaCl) were injected into the NOT through a glass micropipette (tip diameter 30 µm) attached to a Hamilton syringe for labeling purposes.

Slice preparation

Slice experiments were performed 2–5 days after dye injections using standard techniques (Conners et al. 1982; Lohmann and Rörig 1994). Animals were anesthetized with halothane, decapitated, and the brains were placed in ice-cold oxygenated artificial cerebrospinal fluid (ACSF). Coronal slices (recording slices 450 µm, control slices 200 µm) were prepared on a vibratome from a block containing the cytoarchitectonically defined areas 17, 18, and 18a. The slices were maintained at room temperature in oxygenated ACSF for at least 1 h. The slices were then transferred to a submerging chamber (Fine Science Tools) and continuously superfused (1.5 ml/min) with oxygenated ACSF at 34°C. The ACSF was equilibrated at pH 7.4 with 95% O_2 and 5% CO_2 and composed of: 124 mM NaCl, 5 mM KCl, 1.25 mM NaH_2PO_4, 26 mM $NaHCO_3$, 2 mM $MgSO_4$, 2 mM $CaCl_2$, 10 mM glucose (compare Amitai 1994; Lohmann and Rörig 1994).

In control slices the exact localization of the retrograde labeling was confirmed by means of appropriate epifluorescence illuminations. In adjacent recording slices the position of stimulation electrodes and the actual recording sites were chosen by determining the location of fluorescing projection neurons in the control slices.

Stimulation and recording

Intracellular recording and labeling was accomplished using micropipettes filled with 2% biocytin in 2 M potassium acetate solution (60–100 MΩ), as described elsewhere (Lohmann and Rörig 1994). All the recorded signals were fed into the high-impedance probe of an intracellular recording amplifier (Dagan 8100). They were filtered at 5 kHz, digitized at a rate of 10 kHz with a lab interface (CED 1401), and stored for later off-line analysis. The electrophys-

iological properties were characterized by standard techniques (Connors et al. 1982). Input resistance was determined by measuring averaged responses to small hyperpolarizing current pulses that evoked voltage deflections within the linear range of the current-voltage (I-V) curve. Regression was accepted for $r>0.75$ (cf. Lohmann and Rörig 1994). Small hyperpolarizing current pulses (150 ms duration, evoked response less than 10 mV) were used to evaluate the time constant. Spiking behavior was tested in all the recorded neurons by implementing 150-ms depolarizing current pulses (with current amplitudes of up to 2 nA). Spike amplitudes were measured from threshold to peak, and spike widths were measured at half the amplitude of the spikes. The recorded neurons were classified as RS, IB, or doublet-spiking (DS), according to the criteria of Connors et al. (1982), McCormick et al. (1985), and Wang and McCormick (1993) with respect to their responses after depolarizing current pulses. Furthermore, the current threshold for eliciting an action potential (rheobase) was determined by 600-ms-long depolarizing current pulses. The minimal length of a current pulse to elicite a spike (chronaxy) was determined at a current amplitude of twice the rheobase current (Katz 1966). Spike afterpotentials were evaluated using current pulses (pulse duration 150 ms) just above firing threshold (eliciting only one action potential) and with amplitudes set at 1 nA above this threshold (eliciting groups of action potentials). Resting membrane potential was calculated as difference between the intracellularly recorded membrane potential and the extracellular potential upon electrode withdrawal from the cell. Neurons were recorded in the cytoarchitectonically defined areas 17 and 18a. The position of the actual recording site was dependent on the localization of the retrograde labeling.

Intracortical stimulation was performed using an eight-channel stimulation electrode (interelectrode distance 100 μm; Lohmann and Rörig 1994; Lohmann and Algür 1995) consisting of quartz glass-coated platinum-rhodium fibers (Reitboeck 1983), oriented parallel to the cortical laminae either in layer II/III or in layer V. The eight-channel stimulation electrode was inserted only once into every slice in order to avoid damage to the tissue as much as possible. After inserting the stimulation electrode, we tried to impale one neuron close to the first channel of the electrode (ca. 50 μm away) and a second neuron approximately 500 μm away. Stimulation started with the electrode closest to the recorded neuron, where a stimulation current eliciting an excitatory postsynaptic potential (EPSP) of 2–3 mV allowed the EPSP slope to be investigated. This process was repeated sequentially for all the electrodes. The afferent fibers were stimulated by a conventional bipolar electrode (Rhodes Medical; SN 100) placed into layer VI at the border between the gray matter and white matter. Current pulses (50 μs duration) were delivered through these electrodes with a frequency of 0.1–0.3 Hz. The current strength was chosen so that it elicited EPSPs of 2–3 mV amplitude in the recorded neuron. Five responses were recorded; no averaging was performed. The onset and peak latencies, shape, half-width, and slope of each postsynaptic potential were analyzed for every distance between the stimulation and the recording sites. The conduction velocity of the stimulated fibers was determined as the inverse slope of the linear regression line in a latency-distance plot. The EPSP with the highest slope in the five recordings was chosen for the slope versus distance plot and for the onset-latency versus distance plot, because in this case the synapses were assumed to have had an optimal transmitting rate.

Histological procedure

At the end of an intracellular recording session, each neuron was injected with biocytin (Horikawa and Armstrong 1988; Tseng et al. 1991) by means of 100-ms depolarizing current pulses of 1 Hz and 0.5 nA amplitude for 10 min to allow later morphological classification. Each slice was maintained within the recording chamber for 1–2 h to enhance the staining by fast axonal transport. Slices were fixed in 4% formaldehyde in 0.1 M phosphate-buffered saline (PBS) and stored in 30% saccharose in PBS overnight. Slices were resectioned at 50 μm on a freezing microtome, incubated in avidin-conjugated horseradish peroxidase, and reacted with diaminobenzidine (ABC Kit; Vector) according to the method described by Horikawa and Armstrong (1988), except for the fact that the slices were not cleared in ethanol because this would have led to the RLM being destroyed. Sections were examined with a Zeiss Neofluar 100 objective under epifluorescent illumination, either with a rhodamine or a FB filter set. A cell was accepted as prelabeled if at least five fluorescent beads could be counted in its soma. Data from unlabeled neurons presented in this study were only gathered in experiments where back-labeled cells had been successfully recorded. This was done to obtain as little contamination as possible from subcortical projection neurons in this population, and to allow the data from slices to be compared under identical physiological conditions.

Morphological analysis

The following morphological parameters were examined: For all the neurons that were sufficiently filled with biocytin, the number of first- and second-order basal dendrites, the spine density, bouton density, and the extension of the apical dendrite in layer I and the basal dendritic field in layer V were determined. The soma area was determined using the Neuron Tracing System (NTS) 5.14 from Eutectics. Spine density was determined as follows: On selected segments of fairly straight dendrites that were at least 40 μm long, spines were counted under a high-power (Zeiss ×100/1.3) oil-immersion objective. This length was chosen because it allows a direct comparison with the values given by Hübener et al. (1990). This procedure was performed on first-order apical segments at a distance of 300 μm from the soma (in other words, in layer III), on second-order dendrites in layer II that were more than 200 μm below the cortical surface, and on third-order apical dendrites in layer I. A similar procedure was carried out for second-order basal dendrites in layer V, but not for first-order basal dendrites, because their lengths were too variable from cell to cell. Third-order basal dendrites were not analyzed in this way, because the lengths of the segments of these dendrites located in layer VIlayer VI were too variable, depending on whether location of the soma was either more in the upper or more in the lower part of cortical layer V. It is possible, and the results for the apical dendrites confirm this, that spine density depends on the cortical layer through which the dendrites run. Spine numbers counted were corrected following the method used by Feldman and Peters (1979). The counting was performed several times for every type of segment. A three-dimensional (3-D) reconstruction was performed for selected neurons using the following scheme. Neurons were chosen if at first sight they appeared to be completely filled and if their axonal and dendritic trees did not reveal too many cut (or split) ends during reconstruction. With the aid of NTS, this allowed the total axon length, the total number of boutons on the axons counted while tracing the axons, and the total length of basal and apical dendrites to be determined. It was also possible to estimate the total number of spines on these cells.

Intercell distances and nearest-neighbor analysis

Intercell distances from each neuron in one population to any other neuron in the same population were calculated using the appropriate module of the NTS 5.14 from Eutectics. In the same way the distance to the nearest neighbor was calculated.

Data analysis and statistics

Data presented in this paper are given as means±standard deviation (SD) if not otherwise stated. ANOVA and pairwise ANOVA were used to compare data from the different populations. If nothing could be said about the shape of the distribution of the data sample, the nonparametric analog for the one-way ANOVA, the Kruskal-Wallis test, was performed. Differences in either test were regarded as significant at $P<0.05$. The principal component analysis (PCA) was based on a correlation matrix in order to avoid problems due

to the different scaling of the parameters used. All the tests were performed with the statistical software package SYSTAT for Windows 5.03; its modules were tested with standard statistical data sets for computing correctness.

Results

Labeling

In four experiments we succeeded in labeling the NOT and SC in such a way that no diffusion of the dyes into neighboring structures occurred. In one of these animals, both midbrain structures were almost completely filled. Of all the back-labeled neurons, 60.3% project to the SC, 34.6% to the NOT, and 5.1% to both structures. Retrogradely labeled somata were completely restricted to layer V, indicating that probably no callosal fibers had taken up the dyes when the contralateral cortex was penetrated with the injection pipette.

The retrograde labeling after double-labeling SC and NOT thus showed that the corticotectal and corticopretectal neurons form two separate populations with little overlap. The two populations exhibited a distinct pattern within layer V. While SC-projecting neurons show an approximately uniform distribution across areas 17, 18, and 18a, NOT-projecting cells were mainly located at the borders between visual areas 17/18 and 17/18a in the binocular zone of the visual cortex. This fact is demonstrated more clearly in Fig. 2, where a frequency distribution of the intercell distances is plotted. A Poisson distribution could be fitted (r^2=0.97, n=20301) to the pattern of corticotectal cells, indicating a random distribution of this population in layer V. A peak formed at an intercell distance of 50 µm. Corticopretectal neurons showed a bimodal distribution (in this case we were able to use a Gabor-function with r^2=0.92, n=13309). In addition to the peak at 50 µm, a second peak appeared at a distance of 2.5 mm in this distribution. This length equals the distance of areal borders 17/18–17/18a in the rat visual cortex. In the nearest-neighbor analysis of cell distances, both populations exhibited a Poisson distribution with a peak at 50 µm, thus indicating a random arrangement of the neurons within their patches of occurrence.

Electrophysiological results

Intracellular stimulation

One hundred and sixty neurons retrogradely labeled from either the SC or the NOT were intracellularly recorded and stained in 120 slices from 27 experiments. Of these recorded cells, 21 neurons showed retrograde labeling

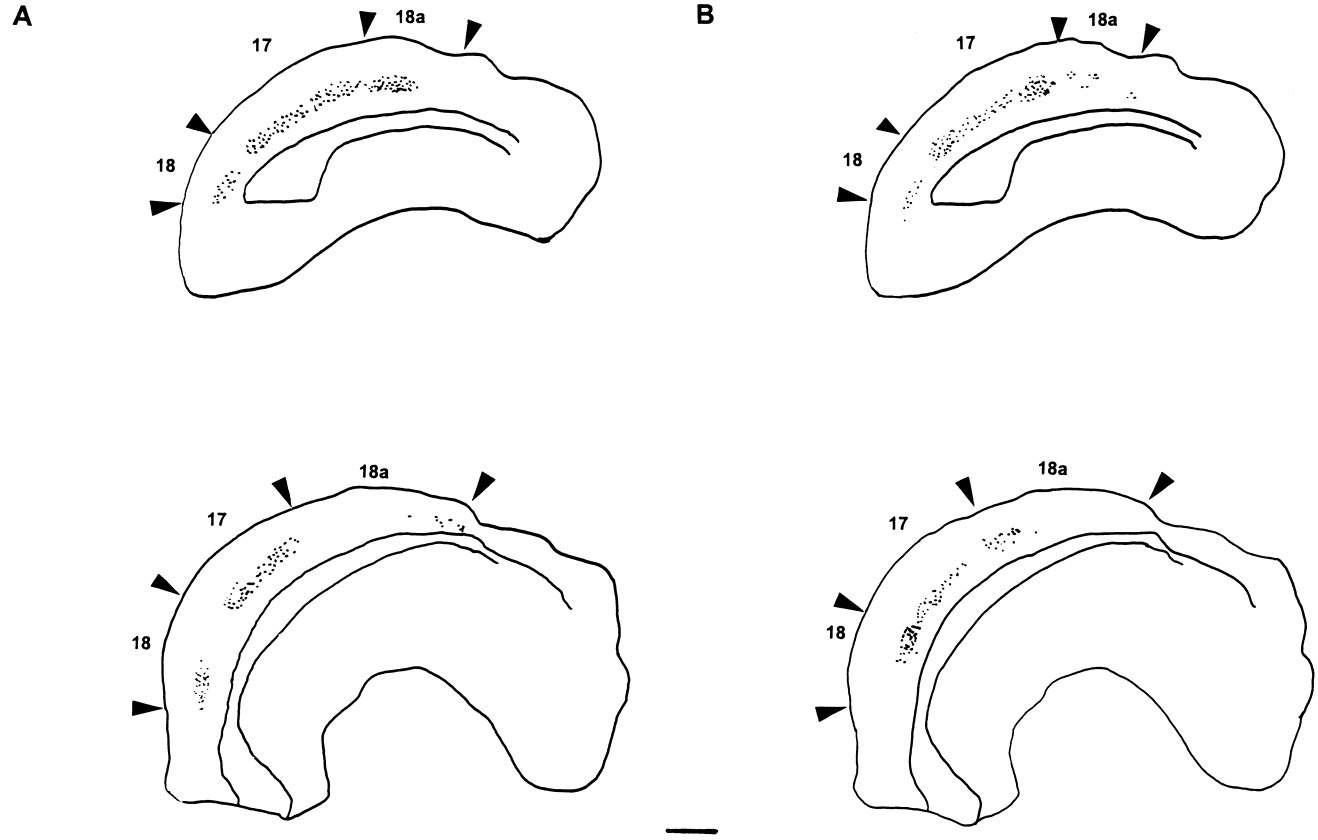

Fig. 1 **A** Reconstruction of the distribution of cortical neurons back-labeled from of the superior colliculus. Note the uniform distribution of the somata. **B** Reconstruction of the distribution of cortical neurons, back-labeled from the nucleus of the optic tract. Note the non-uniform distribution of the somata, with patches at the areal borders 17/18 and 17/18a. *Arrowheads* mark cortical area borders adapted from Zilles (1985). *Scale bar* 1 mm

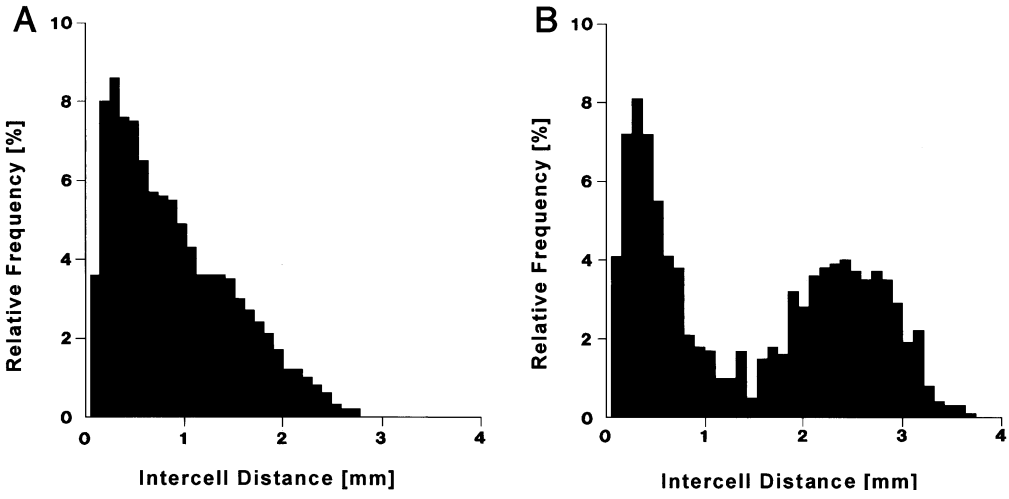

Fig. 2 **A** Frequency distribution of intercell distances for corticotectal neurons. A Poisson distribution could be fitted with r^2=0.97, indicating that this population is randomly distributed in layer V. **B** Frequency distribution of intercell distances for corticopretectal neurons. A Gabor function could be fitted with r^2=0.92, suggesting that this population is not purely randomly distributed. The *x*-axis repesents the distance between two cells in millimeters

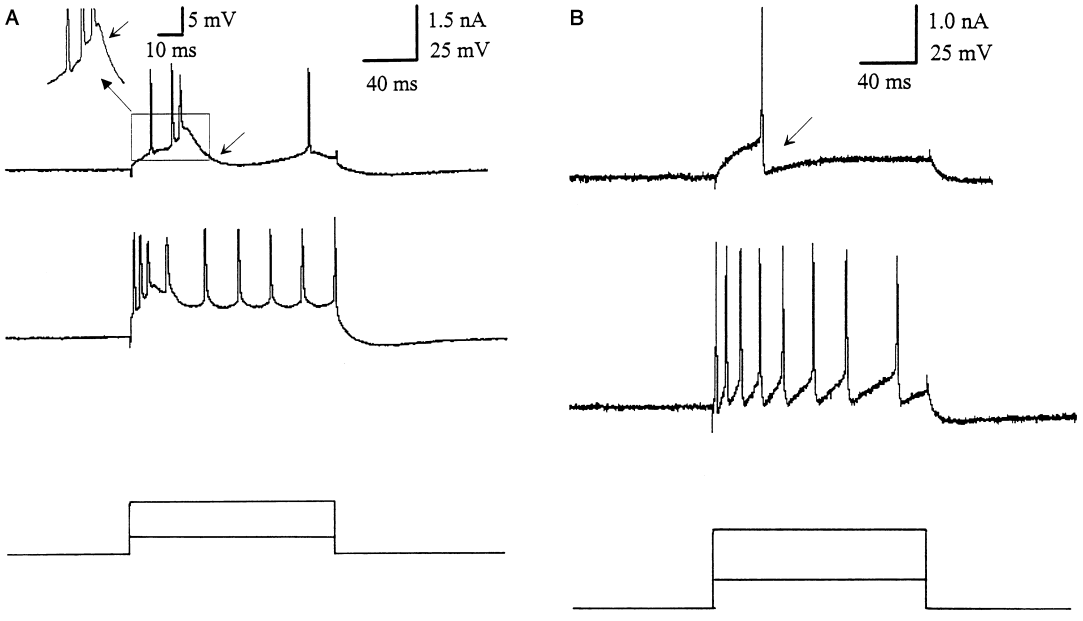

Fig. 3 **A** nucleus of the optic tract (NOT)-projecting neuron with intrinsically bursting (IB) characteristic. The response to a small, depolarizing current pulse shows a fast afterhypolarizing potential (ahp) after the first spike (cf. *inset*). The neuron responds to a higher depolarizing current with a burst of four spikes, followed by a repetitive firing until the end of the current pulse. **B** NOT-projecting neuron with regular-spiking characteristic, which shows strong and fast ahp (*arrow*). It was not possible to switch this neuron to an IB mode

from the NOT and 15 from the SC. The remaining neurons were not back-labeled from either of the two structures and were therefore not included in this study. Neurons prelabeled from both structures were not recorded. In all recorded cells there were sufficient responses to current pulses to warrant classification of their spiking behavior. All the prelabeled neurons could be classified as large layer V neurons with an apical dendrite that reached layer I and arborized there in a tuft (for a detailed morphological analysis, see Morphological results). Physiological data from 19 NOT-projecting and 14 SC-projecting neurons were sufficiently complete to be suitable for detailed quantitative analysis. Membrane potential for corticopretectal neurons was –70.4±5.8 mV (n=21), –68.5±4.7 mV (n=15) for corticotectal cells, and –69.9±4.7 mV (n=56) for unlabeled pyramids. Fourteen NOT-projecting and nine SC-projecting neurons were recorded in area 17, the remaining 13 neurons in area 18a.

Based on their spike-firing pattern after depolarizing current pulses, two groups of identified corticopretectal neurons could be distinguished: (1) 16 cells could be classified as IB, because they exhibited a burst with at least three spikes at higher current pulses, followed by some regularly spaced single spikes; (2) five neurons could be classified as RS with prominent frequency adaptation of the spikes to the intracellularly applied current pulse (see Fig. 3). In the same way, three groups could be placed in the corticotectal group: (1) 12 cells could be classified as IB, (2) two cells as DS, (3) one neuron as

Table 1 Physiological properties of layer V projection neurons. Note that no major differences occur in the specific afterpotentials in the two populations (percentage values do not add up to 100 per population, because mostly there was more than one afterpotential present for an individual neuron) (*SC* superior colliculus, *NOT* nucleus of the optic tract, *fahp* fast afterhyperpolarizing potential, *fadp* fast afterdepolarizing potential, *sahp* slow afterhyperpolarizing potential, *sadp* slow afterdepolarizing potential)

	Unlabeled neurons (*n*=56)	SC-neurons (*n*=14)	NOT	
			Large (*n*=14)	Slender (*n*=5)
Membrane potential (mV)				
Mean	–69.7	–68.5	–67.7	–71.8
±SD	4.5	4.7	5.5	7.9
Input resistance (MW)				
Mean	40.7	42.5	38.8	56.5
±SD	17.7	18.1	17.7	17.9
Spike height above threshold (mV)				
Mean	59.2	56.5	57.2	62.2
±SD	6.2	7.2	6.5	7.3
Spike duration at half amplitude (ms)				
Mean	0.87	0.81	0.81	0.62
±SD	0.32	0.23	0.35	0.13
Chronaxie (ms)				
Mean	12.2	13.9	14.9	
±SD	7.9	8.4	5.5	
Rheobase (nA)				
Mean	0.34	0.3	0.28	0.35
±SD	0.21	0.12	0.09	0.04
Time constant (ms)				
Mean	8.0	7.3	10.0	8.1
±SD	2.3	2.6	3.1	1.8
fahp				
n	13/21	8/14	9/14	2/5
%	60	50	60	40
fadp				
n	10/21	6/14	6/14	3/5
%	50	40	40	60
sahp				
n	15/21	14/14	10/14	3/5
%	70	100	70	60
sadp				
n	10/21	6/14	7/14	3/5
%	50	40	50	60

None of the above parameter data showed significant differences in the ANOVA at the 5% level of significance

RS. It was not possible to switch the RS neuron to an IB firing characteristic (neither by hyperpolarizing, nor by depolarizing the membrane). To our knowledge this is the first report of a corticotectal cell with RS behavior. The firing characteristics of all the IB-type cells could be switched between the IB and RS modes, by depolarizing the membrane potential (data not shown).

In an attempt to come up with electrophysiological parameters in which corticotectal and corticopretectal neurons showed statistically significant differences, we examined subthreshold properties such as membrane potential, membrane resistance, and time constant, and threshold parameters such as spike amplitude, spike width, chronaxie, and rheobase (see Table 1). In none of these parameters could significant differences between the two populations be found in the ANOVA.

The primary apical dendrite of a subpopulation of five NOT-projecting cells exhibited a distinct morphology. Their dendrites were very thin (diameter less than 2 μm), with a tuft diameter of about 250 μm. These cells also showed a higher membrane resistance, a slightly higher firing threshold, and a slightly smaller time constant than the large corticopretectal neurons (see Table 1). In their firing pattern, three of them could be classified as RS, the other two as IB.

In addition we looked at particular sequences of spike afterpotentials (inset in Fig. 3). An NOT-projecting neuron with an IB characteristic is shown in Fig. 3A. At low current pulses, the neuron displayed a group of three spikes riding on an underlying depolarization, which is probably mediated by Ca^{2+} (Amitai et al. 1994). Each action potential was followed by a fast afterhyperpolarization (fahp), 2 ms long, and a slow afterdepolarization (sadp), 15 ms long. The whole sequence was followed by a long-lasting, slow afterhyperpolarization (sahp). When the current pulse amplitude was increased, fahp could no longer be detected after single spikes, although it persisted after the action potentials of the burst. The response of a corticopretectal neuron with RS characteristic is shown in Fig. 3B. This cell generated individual spikes that lasted less than 0.5 ms and a high-amplitude fahp after each spike, which is normally thought to be a feature of GABAergic interneurons. In contrast to those GABAergic interneurons, however, this corticopretectal cell showed a clear adaptation in spike frequency (McCormick et al. 1985;

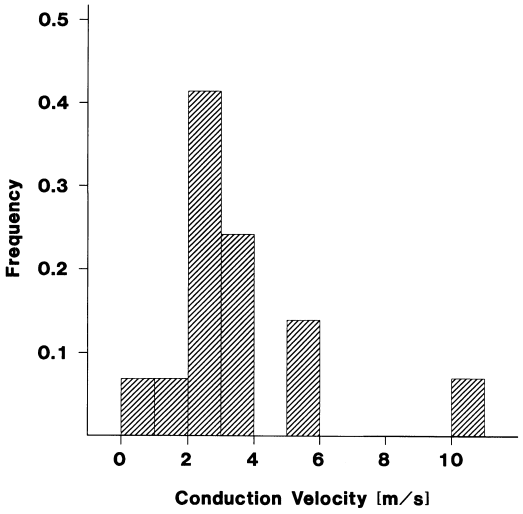

Fig. 4 Frequency histogramm of 35 measured conduction velocites after stimulating layer II/III. Median value was found to be 0.29 m/s (SD 0.17 m/s)

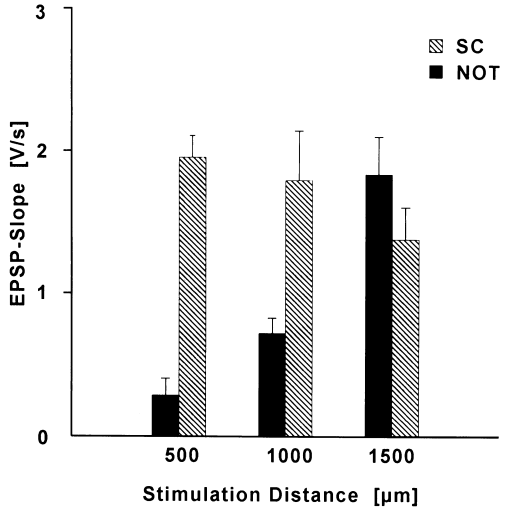

Fig. 5 EPSP slope versus stimulation distance in layer II/III for superior colliculus (*SC*)- and NOT-projection neurons. For SC-projection neurons, note the high EPSP slope at short and middle stimulating distances and the decrease in EPSP slope at stimulation sites further than 1000 µm away. NOT-projection neurons exhibited the steepest EPSP slope at stimulation distances of 1500 µm. Data presented for six SC and six NOT neurons. *Error bars*, SEM

Connors and Gutnick 1990; Agmon and Connors 1992). Such behavior could be seen in two corticopretectal neurons. The same afterpotential sequences as described above for corticopretectal neurons could be detected in corticotectal neurons (see Table 1).

Extracellular stimulation

In the electrophysiological parameters examined so far, no significant differences between the two populations of projection neurons could be found. Therefore, we decided to study the connectivity of the neurons within the surrounding cortical network and tested this by means of intracortical microstimulation. For these tests we used the eight-channel multielectrode introduced by Lohmann and Rörig (1994) to stimulate inputs to the recorded neurons from several lateral distances. The current amplitudes applied ranged from 100 to 800 µA. The current strength necessary to elicit responses of the same amplitude increased with the stimulation distance in a linear way, r^2=0.75 (n=44). A frequency histogram is shown in Fig. 4 for all the measured conduction velocities following stimulation in layer II/III. The median of the conduction velocities was found to be 0.29±0.17 m/s (n=35), which is very close to values reported by Lohmann and Rörig (1994). The median for corticotectal neurons was found to be 0.29±0.16 m/s (n=10) and for corticopretectal cells, 0.28±0.17 m/s (n=9).

To study the effectiveness of the extracellular stimulation from different cortical locations, we also compared the slopes of the primary EPSPs as a function of the intracortical stimulation distance (EPSPs with steeper slopes elicite spikes more effectively; see Nicoll et al. 1993 for a discussion of this problem). When cortical layer II/III was stimulated, we found that SC-projecting neurons were more effectively stimulated from distances in close and middle ranges. At stimulation sites up to 1000 µm, corticotectal cells show median values for EPSP slopes between 2 and 1.7 V/s, compared with values between 0.4 and 0.7 V/s for corticopretectal neurons. For stimulation distances between 1000 and 1500 µm, SC-projecting neurons showed slopes of less than 1.5 V/s, but median EPSP slopes of NOT-projecting neurons were found to be 2 V/s (see Fig. 5). These differences could not be observed when electrical stimulation was applied to cortical layer V (data not shown).

Principal component analysis

As demonstrated so far, no parameter alone could serve as a classification parameter on a single neuron level. For this reason a principal component analysis was performed to achieve a simultaneous comparison of multiple parameters. EPSP slopes could not be used in this analysis, because the number of tested neurons was too small (n=6 for both populations) to be included.

With time constant (36%), membrane resistance (26%), rheobase (24%), and membrane potential explaining 14% of the observed variability in the data, no further reduction in the dimensionality was possible (all four parameters were necessary to explain more than 90% of the variability of the data). We therefore conclude that there is no additional hidden information that could help to classify the members of these neuronal populations. Except for the parameter time-constant that explained more than one-third of the variability of the data, none of the parameters explained more than the statistical mean of 25% variability (100% variability divided by four parameters).

Table 2 Counts of primary and secondary basal dendrites. Note that no differences could be observed between the two populations

Projection target	Neurons (*n*)	Primary basal dendrites (*n*)		Secondary basal dendrites (*n*)	
		Mean	±SEM	Mean	±SEM
SC	13	5.1	0.3	9.5	0.6
NOT	18	4.9	0.3	9.2	±0.5

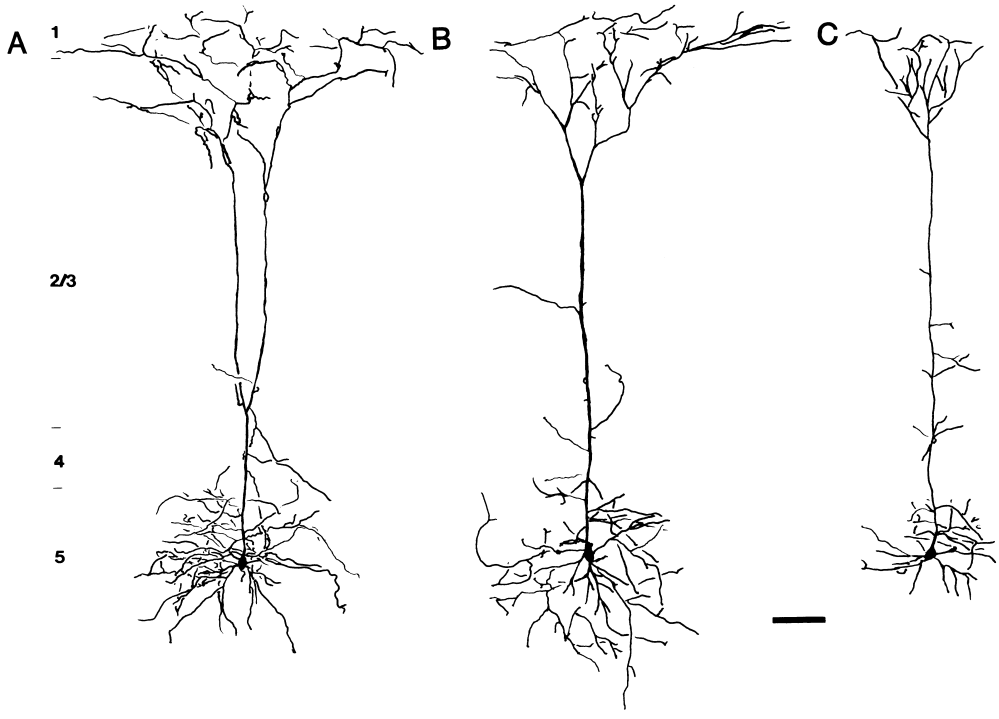

Fig. 6 **A** Two-dimensional (2-D) camera-lucida reconstruction of a NOT-projecting cortical neuron, with an apical dendrite bifurcating in layer III (*3*). The soma is located in layer V (*5*), while the apical dendrite reaches layer I (*1*) and arborizes there in a tuft. **B** 2-D camera-lucida reconstruction of a NOT-projecting cortical neuron. The soma is located in layer V, while the apical dendrite reaches layer I and arborizes there in a tuft. **C** 2-D camera-lucida reconstruction of a NOT-projecting cortical neuron. Note the thin apical dendrite and the sparse arborizations in layers I and V. *Scale bar* 100 µm

Morphological results

Soma area

Hübener et al. (1990) have shown that corticotectal neurons in cat do have significantly larger somata than corticocortical cells. In our sample we were not able to confirm these results for the rat. SC-projecting neurons possessed a mean soma area of 163±51 µm^2 (*n*=15), NOT-projecting neurons attained a value of 152±45 µm^2 (*n*=21), and unlabeled neurons (which should constitute a high percentage of corticocortical neurons; see Materials and methods) had soma areas of 159±44 µm^2 (*n*=25). These differences were not significant in the ANOVA at the 5% level of significance.

Basal dendrites

Counting of first- and second-order basal dendrites is an easy way of determinig classification parameters (Hübener et al. 1990). No differences between the two populations could be observed in our study (cf. Table 2). Also the horizontal extensions of the basal dendritic fields (366±52 µm, *n*=12, for corticotectal neurons; and 345±82 µm, *n*=16, for corticopretectal cells) were found to be similar. The total length of basal dendrites was determined for eight 3-D reconstructed neurons. For corticotectal neurons it amounted to 5288±1331 µm (*n*=3) and for corticopretectal cells, 6447±1441 µm (*n*=5). These differences were not significant at the 5% level of significance in the Kruskal-Wallis test.

Apical dendrites

The diameter of the proximal part of the apical dendrites (50 µm away from the soma) of corticotectal neurons was, on average, 3.2±0.5 µm (*n*=15). While most of corticopretectal neurons reached similar values (3.1±0.5 µm, *n*=16; see Fig. 6A, B), five neurons recorded in area 17 only reached values of 1.8±0.4 µm (see Fig. 6C). This characteristic only correlated with one morphological parameter. In layer I, corticotectal neurons showed a prominent tuft with a mean lateral extension of 277±115 µm (*n*=12). The horizontal lateral extension of the apical dendrite never exceeded the extension of the basal dendrites. In contrast, corticopretectal neurons exhibited a much larger tuft in layer I. These neurons reached a horizontal extension of up to 800 µm, on average, 502±128 µm (*n*=14).

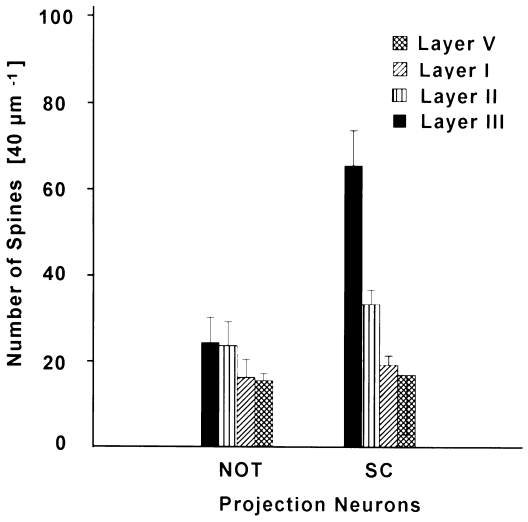

Fig. 7 Comparison of spine density of corticotectal and corticopretectal neurons for different dendritic segments. Note that no significant statistical differences between the two populations in cortical layers I and V can be observed. In contrast, differences emerged when spine densities in cortical layers II and III were compared. *Error bars*, SEM

Table 3 Spine counts for five three-dimensionally reconstructed projection neurons. Despite their lower spine density on dendrites located in layer II/III, corticopretectal neurons (*NOT-1*, *NOT-2*) did not necessarily possess fewer spines than corticotectal neurons (*CS-1*, *CS-2*, *CS-3*). Both populations show the total bandwidth of spine counts reported by other authors. Both populations also exhibit the same number of spines on the basal dendrites

Spine counts	CS-1	CS-2	CS-3	NOT-1	NOT-2
Apical dendrite	2.040	5.500	1.300	5.000	700
Basal dendrite	1.400	1.500	1.300	1.500	1.300
Total	3.440	7.000	2.600	6.500	2.000

The five corticopretectal neurons with thin apical dendrites on average showed smaller tufts in the lateral extension, comparable with those found in corticotectal cells (mean 248±82 µm). The difference in lateral extension of the apical dendrite between the corticotectal and corticopretectal neurons was significant at $P>0.001$ in the ANOVA.

Spines

When the spine density of the two projection neuron groups was compared, differences emerged, depending on in which segment or in which layer the spine densities were compared. No differences could be detected in the basal dendrites in layer V, in the oblique dendrites (apical dendrites arborizing in layer V), or in the third-order apical dendrites located in layer I (see Fig. 7). Differences could be observed when dendrites located in the cortical layer II/III were compared. Here corticotectal neurons revealed a much higher spine density than corticopretectal cells. On their first-order apical dendrites in layer III, corticotectal neurons possessed, on average, 65±28 spines per 40 µm (n=13), compared with corticopretectal neurons with 24±18 spines per 40 µm (n=18). On second-order apical dendrites, corticotectal neurons had, on average, 33±11 spines per 40 µm (n=12), compared with corticopretectal neurons with 24±17 spines per 40 µm (n=17). In both cases the 5% level of significance was reached (see Fig. 7) in the ANOVA.

The total number of spines was estimated for three corticotectal and two corticopretectal 3-D reconstructed neurons. Despite their lower spine density on some segments, corticopretectal neurons did not necessarily possess fewer spines than corticotectal cells, as is demonstrated in Table 3.

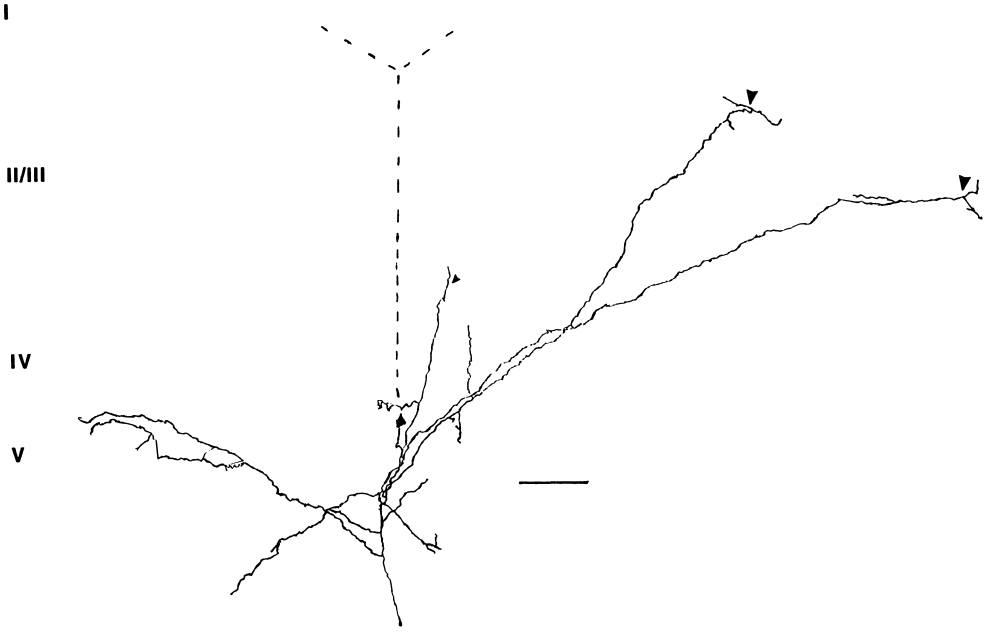

Fig. 8 Three-dimensional reconstruction of the intracortical axon collaterals of a corticotectal neuron. Apical dendrite is represented by a *dotted line*. Note that near each neuron's apical dendrite no ascending collaterals are found (the collateral marked by a *small arrow* lies in front of the plane of drawing). Note also the wide extension of these ascending collaterals (marked by *arrows*)

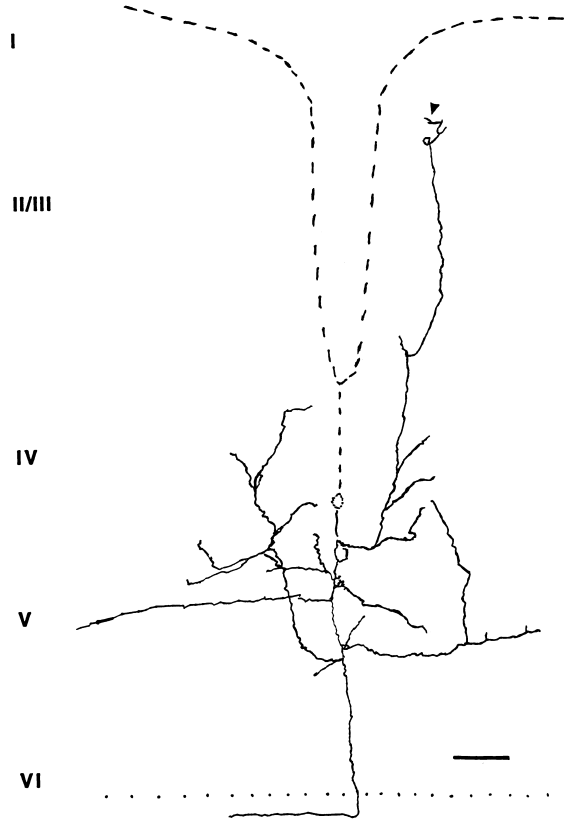

Fig. 9 Three-dimensional reconstruction of the intracortical axon collaterals of a corticopretectal neuron. The bifurcating apical dendrite is represented by a *dotted line*. Note that the ascending collaterals stay very close to their own apical dendrites. One collateral that nearly reaches layer I is marked by an *arrow*. When the descending axon reaches the white matter, it makes a 90° turn and runs parallel with the other fibers, continuing to form boutons

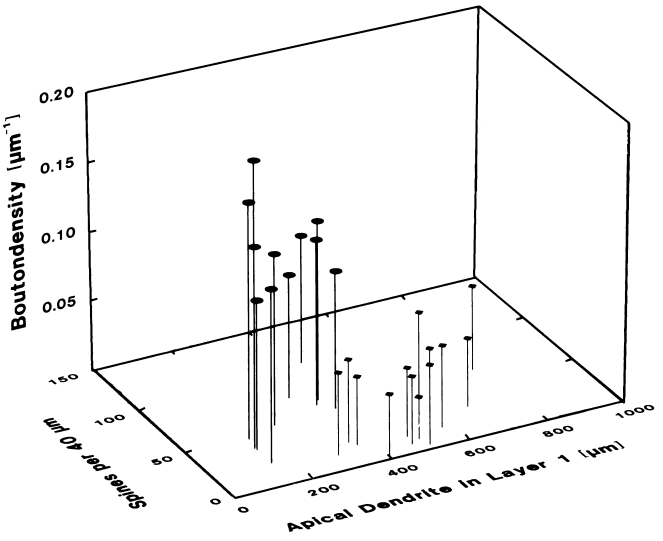

Fig. 10 Spine density of corticotectal (SC) and corticopretectal (NOT) neurons, and bouton density as a function of the extension of their apical dendrite in layer I. NOT-projecting neurons are clustered in the *lower right quarter*, while SC-projecting cells are concentrated in the *upper right*. Note that no overlap between the two populations occurred

Axons

In contrast to dendrites and spines, no differences between the two populations of projection neurons could be observed when the number and length of the axon collaterals in cortical layers V and VI were compared. Both populations had long horizontal collaterals reaching extensions of up to 1 mm. When the arborization of the axon collaterals in layer II/III was compared, a different picture emerged. Corticotectal neurons exhibited long ascending collaterals that entered cortical layer II/III at a distance of 200 µm from their own first-order apical dendrite. They often did so at an angle of 45°. Similar to the collaterals in layer V, these collaterals reached lateral extensions of 1 mm. In contrast, such wide arborizations could not be observed for corticopretectal neurons. Their ascending collaterals stayed very close to their own first-order apical dendrite at a lateral distance of 10–150 µm. Mostly, they branched from other collaterals at an angle of 90° in layer V projecting to the supragranular layers. Ascending collaterals from both populations reached cortical layer I. The differences in the arborization pattern were accompanied by differences in the total axonal length. For three 3-D reconstructed corticotectal neurons the mean length was 8571±2927 µm. An example of the axonal arborization of a corticotectal neuron is shown in Fig. 8. Five 3-D reconstructed corticopretectal neurons were measure in the same way. The branching patterns of these five neurons revealed no differences in frequencies of branch orders or maximal lengths of collaterals. The total axonal length in this group was, on average, 4970±2088 µm. While the largest axonal tree of a corticotectal neuron was 11810 µm, the corticopretectal neuron with the largest tree only reached 7350 µm. A typical example of the axonal arborization pattern of corticopretectal neurons is shown in Fig. 9.

Boutons

On average, corticotectal neurons showed a bouton density of 13 boutons per 100 µm in all the axonal segments, while for corticopretectal cells a mean bouton density of six boutons per 100 µm was observed. Consequently, corticotectal neurons possessed up to 4 times more intracortical boutons than corticopretectal cells (1700 boutons for corticotectal cells and 450 boutons for corticopretectal cells) owing to their larger axonal trees and their higher bouton density.

The power of these morphological parameters as a classification tool is demonstrated in Fig. 10. It was possible to separate both populations completely if the extensions of the apical dendrite in layer I, the bouton densities, and the spine densities in layer III in first-order apical dendrites were plotted against each other. While the NOT-projecting neurons clustered in the lower right of

the graph as a result of their huge apical dendrites and low spine density, SC-projecting cells were grouped in the upper left of the graph, owing to their high spine density in layer III, high bouton density, and the small lateral extension of their apical dendrite in cortical layer I.

Discussion

We characterized corticopretectal and corticotectal cell populations in the visual neocortex of the rat. The main finding of this study is that NOT-projecting and SC-projecting neurons, while being biophysically similar, nevertheless can integrate and transmit different aspects of cortical visual information to their target structures. This is suggested by the differences in their morphology (spine density and extension of tuft) and by the differences in their responses to microstimulation in layer II/III. The results of the intracellular stimulation experiments suggest that both populations exhibit a significant functional diversity with respect to the intrinsic membrane properties that control their spiking behavior. Furthermore, variations between these two populations, either in electrophysiological or morphological parameters, are mainly observed in supragranular layers. Responses to intracortical microstimulation and spine counts differ in cortical layer II/III, the apical denrite tuft extension varies in layer I.

For corticotectal neurons and callosal projecting cells (CC-cells), Kasper et al. (1994) have demonstrated that both cell populations can be separated by biophysical and morphological parameters (SC-projecting neurons: large neurons, soma always located in layer V, tuft in layer I, IBs, low input resistance, low time constant; CC-cells: slender morphology, soma located in layers II/III and V – if in layer V, the apical dendrite does not reach layer I – RSs, higher input resistance, high time constant).

Before looking at the results of our experiments in greater detail and comparing them with previous studies, we will first critically evaluate the methods used. Everyone implementing dyes for retrograde labeling encounters the problem of dye uptake by fibers en passant. The dyes used in this study allegedly minimize this problem as far as possible (for FB, see Kuypers et al. 1980; for RLM, see Katz et al. 1984). Therefore it is unlikely that the retrograde labeling will be contaminated, owing to the proximity of the NOT to the brachium of the SC. Furthermore, RLMs are known to have a small diffusion area. In every experiment performed, we verified that no dye diffused in the diffusion zone of the other dye. In cases where this occurred, the results were not included in this study. This is the main reason why only a small number of experiments labeling both SC and NOT were considered successful. The qualitative results confirmed the well-known fact that projection neurons to the mesencephalon are located exclusively in layer V of the visual cortex (Klein et al. 1986; Schofield et al. 1987; Hübener and Bolz 1988, Hallman et al. 1988; Koester and O'Leary 1992; Wang and McCormick 1993; Kasper et al. 1994). Our counts of the proportion of neurons (only determined in animals in which both structures were almost completely filled) that were back-labeled from both the SC and NOT agree with the findings made by Mader (1987), who reported values of between 15% and 20% of cortical NOT-projecting cells that also project to the SC for the cat.

Resting membrane potentials and membrane time constants are similar to those reported by Kasper et al. (1994). The input resistances in our sample are higher, probably due to the fact that neurons with very thin apical dendrites projecting to the NOT are included in our sample. Such types of neurons, which are known to have a higher input resistance (Mason and Larkman 1990), are missing from Kasper's sample. The conduction velocities observed after extracellular microstimulation are nearly identical to the values reported by Lohmann and Rörig (1994). From all this we conclude that our slices were in a good physiological condition. Care was taken to stimulate the projection neurons from the same cytoarchitectonically defined area as the one in which they were located, hence the stimulation should be considered to be intracortical (except for stimulation sites more than 1500 μm apart). The mean values of conduction velocities of 0.29 m/s (see Fig. 4) support this notion (Lohmann and Rörig 1994). If the stimulated axons passed through the white matter they would have been partly myelinated and conduction velocities would have been higher.

When preparing slices of a certain thickness, 450 μm in our case, long dendritic and axonal processes consequently are lost. In particular, the long horizontal axon collaterals and the long dendritic tufts in layer I are likely to be severed. But this only has an effect on the total axonal and dendritic length and the maximum lateral extensions of the axonal and the dendritic trees. Therefore, the results of the present paper should be regarded as a qualitative description of the differences in the arborization patterns of the neurons (dendritic and axonal) and not as quantitative (absolute) measures. A study implementing intracellular recordings in vivo would, of course, be optimal (as performed by Mader 1987). Furthermore it is not likely that the differences between the two populations are due to the dendritic/axonal trees not being completely filled. If this was the case one would have to accept the hypothesis that the filling of the dendritic tree was incomplete in all corticotectal neurons, while it was complete for the corticopretectal neurons. This hypothesis would also imply that filling axonal collaterals in cortical layer V of a corticopretectal neuron had been complete, or that it had not been severed by the slicing procedure, and the filling was incomplete for axonal collaterals in layer II/III. However, if we keep these results in mind, the presented data are nevertheless clear enough to draw the following conclusions. The values given for the total axonal length might be underestimated and therefore have to be corrected, but for both populations. After all, these limitations did not affect parameters such as the soma area, spine, and bouton density.

Membrane parameters

Our results clearly demonstrate that the subcortically projecting cells in layer V of a rat visual cortex constitute a heterogeneous population with regard to their electrophysiological properties. This confirms data presented by Tseng and Prince (1993) and Lohmann and Rörig (1994) showing that there are large layer V pyramids that could be classified as RS. Thus, our observation contradicts the results reported by Chagnac-Amitai et al. (1990), Larkman and Mason (1990), and Kasper et al. (1994) that all large layer V neurons or all corticotectal cells can be classified as IB. It was not possible to identify the projection neurons only according to their electrophysiological response mode, even though we reached a much higher resolution in prelabeling midbrain structures compared with other investigators. Wang and McCormick (1993) and Kasper et al. (1994), for example, injected either many small or a few large amounts of tracer into the SC to obtain strong back-labeling in the visual cortex. With this procedure they most likely also prelabeled the various pretectal nuclei close to the SC, which alone produced a heterogeneous population of prelabeled neurons. According to Hallman et al. (1988), about 60% of corticotectal neurons in rats also project to the pons, and Klein et al. (1986) reported that about half of all corticotectal neurons in hamsters also project to the lateral posterior nucleus. Owing to the existence of multiple targets and the wide variety of possible information needed by the target structures, a clear-cut anatomical-physiological correlation is difficult to prove based on such a population as a whole. Even when a principal component analysis was performed as a clustering method, no correlation was possible. Moreover, no typical spike afterpotential sequence could be found for the two populations of projection neurons.

We therefore conclude that the response properties of the neurons to intracellularly applied current pulses do not allow these two populations to be separated. Our data agree with results of Tseng and Prince (1993), who also found that corticospinal neurons constitute a very heterogeneous group, and Lohmann and Rörig (1994), who found no strong correlation between the morphology and electrophysiology of neurons in rat visual cortex. We were also able to confirm the results of Chen et al. (1996a, b), who succeeded in demonstrating that large layer V pyramids of cat motor cortex do show narrow spikes with a fahp, something which we found for two corticopretectal neurons (see Fig. 3B). In addition, the classification of neurons as IB, DS, or RS is not as easy as one might wish. Our impression is that the spike discharge behavior of both populations is better described as "... a continuum of variations...," as stated by Connors and Gutnick (1990). The fact that Silva et al. (1991a, b) and Tseng and Prince (1993) introduced another classification based on the response pattern and the different sequences of afterpotentials makes this problem even more complicated. But if the populations are compared per se, the corticopretectal population contains a much higher proportion of RS neurons (25%) than the corticotectal population (7%). In addition, none of the corticopretectal neurons could be classified as DS, in contrast to 13% of the corticotectal neurons.

The finding that concludes there are no different afterpotential sequences for the two cell populations, (cf. Table 1) suggests that these projection neurons do not possess special ion channels determined by their projection target. It is still possible that differences in channel equipment could be detected using pharmacological methods and patch-clamp techniques. Such a suggestion is supported by the results of Solomon et al. (1993), who reported a projection target-specific expression of an inward current with a fast and slow component in acutely dissociated cell cultures.

Intracortical microstimulation

The linear correlation between applied current amplitude and stimulation distance implies that in the visual cortex of the rat there is not only a homogenous distribution of fiber types but also a decline in intercellular connectivity with increasing intercell distance (Lohmann and Rörig 1994).

The data of the intracortical microstimulation also suggest that, despite the similar electrophysiological properties of single cells, the connectivity within the surrounding cortical network of the two populations certainly differs. Similar onset latencies for both populations show that these disparities are not a result of different fiber types connecting the two populations. Even the shorter onset latencies in NOT-projection neurons when the lateral stimulation distance exceeds 1500 μm is probably due to a partial myelination of the stimulated fibers traveling through the white matter. In this case it would be more appropriate to speak of an interareal stimulation.

Nicoll et al. (1993) demonstrated that EPSPs with steep slopes are generated nearer to the soma than EPSPs with low slopes. If these results are applied to our findings for different EPSP slopes dependent on the stimulation distance for the two projection populations, they reveal differences in the physiological as well as the anatomical embedding of corticotectal and corticopretectal neurons in cortical layer II/III. Fibers originating nearby and at midrange distances from recorded corticotectal neurons terminate closer to the soma and are therefore more effective in eliciting an action potential in the postsynaptic neuron than fibers originating from locations further away. For corticopretectal neurons the situation is reversed; here fibers emanating from locations far away terminate closer to the soma than fibers originating from sites nearby.

Morphology

Our morphological data differ slightly from previous reports. The findings of Hübener et al. (1990) for the cat,

namely that corticotectal neurons mainly possess large somata, could not be confirmed by our results for the rat. These authors reported a range of soma areas of 110–300 μm^2. This is consistent with our data, but their sample exhibits a clear shift to higher values, resulting in a mean value of 203 μm^2, compared with the mean value of 163 μm^2 in our findings. Our data are very close to the ones of 164 μm^2 for the hamster reported by Klein et al. (1986). No differences in soma area between the projection neurons and the unlabeled neurons could be found, the latter mostly consisted of corticocortical neurons. In the cat, it is perhaps necessary to transmit the information along thicker axons, owing to the larger distance between the cortex and the SC. This would correlate with the larger somata reported by Tseng and Prince (1993). Nevertheless, Hübener et al. (1990) themselves stated "...that at least in the cat and rat visual cortex, cell body size is not a very useful parameter for the classifications of the neurons."

Our measurements of spine density also differ from several previous reports. Larkman (1991c) reported values of 15000 spines for large layer V neurons. This is nearly twice the number we estimated. There might be several reasons for this discrepancy. First, our method of estimating spines definitely underestimates the total number, because we integrated large parts of the dendritic tree. Second, there are probably differences between the strains of rats used in the two studies that might account for the results observed. We used Long-Evans hooded rats (60 days old), while Larkman (1991, a,b,c) used young (30 days old) Wistar rats. Third, corticotectal neurons might not be the neurons with the highest density of spines. The latter view is supported by results presented by Hübener et al. (1990). Their estimations for SC-projecting neurons of the cat range from 29 to 10000 spines. This result is much closer to our data, especially if one recalls their method of labeling the SC, which results in the pretectum being labeled, too. Possibly for the same reason, Hübener et al. (1990) were unable to establish the clear relationship between the projection target and morphology of the axon collaterals that we were able to observe. Despite this, the estimations of total spine counts shown in Table 3 indicate that corticopretectal neurons do not necessarily possess fewer spines than corticotectal neurons, but that they are distributed differently along the dendrites.

The question now arises as to why corticotectal and corticopretectal neurons exhibit such a distinct spine distribution? Müller and Connor (1991) and Guthrie et al. (1991) were able to demonstrate that the internal Ca^{2+} concentration of each individual spine could be regulated independently of the Ca^{2+} concentration of the mother dendrite. This implies that the cell is able to regulate the efficiency of each synapse. With their numerous spines in layer II/III, corticotectal cells should therefore be able to weigh the incoming information from these layers according to the actual state of the surrounding cortical network by regulating the internal Ca^{2+} concentration in the spines. Together with their small tufts, this should enable the neurons to collect information with high spatial resolution in the cortical map of the visual world. This is in line with the results of the intracortical microstimulation, where corticotectal neurons were most effectively driven by stimulation sites nearby. In contrast, corticopretectal neurons with their small number of spines in layer II/III either receive much less information from the supragranular layers than corticotectal neurons or their inputs go directly on to the dendrites so that they are unable to weigh the incoming information separately. To solve these questions, an electron microscopic study would have to be performed (which was not within the scope of this study).

Other differences have been observed in the dendritic morphology of the two populations. With their huge dendritic arborization in cortical layer I, corticopretectal neurons should be able to collect information from a large part of the visual field; particularly if one recalls that Burkhalter (1989) and Olavarria and Montero (1989), working with the rat, and Felleman and van Essen (1991), with cat and monkey, all demonstrated that most feedback connections from higher visual areas tend to terminate in cortical layer I, because they generally have larger receptive fields. Therefore, corticopretectal neurons should mostly process global (visual) information.

When we take a look at the axonal trees, no differences between the two populations are observed in their arborization in cortical layers V and VI (as for the basal dendritic tree, too). Differences do occur in cortical layer II/III. This is also consistent with the results of the intracortical microstimulation, where no differences between the two populations can be observed during stimulation of layer V. Therefore, it is likely that the different forms of integrations that the two populations might have to perform are done in cortical layer II/III.

There is a problem in interpreting the possible function of the five corticopretectal neurons with a thin apical dendrite. It is unlikely that the characteristics of these neurons are artifacts. Only corticopretectal neurons in area 17 exhibited such a morphology. In fact, neither NOT-projecting neurons in area 18a nor any SC-projecting cells (either in 17 or in 18a) had such a morphology. Furthermore, these neurons with thinner apical denrites possessed a higher membrane resistance (56 MΩ compared with 38 MΩ in the other NOT-projecting neurons). These neurons resemble, in the appearence of their dendritic trees, the "slender" corticocortical neurons presented by Hübener and Bolz (1988) and Kasper et al. (1994).

A schematic presentation of corticotectal and -pretectal neurons is given in Fig. 11 (camera lucida drawings of corticotectal neurons can be found in: for the rat, Schofield et al. 1987; Kasper et al. 1994; for the cat, Hübener and Bolz 1988).

When spines and boutons are regarded as the light-microscopic analogs of synaptic contacts (see Braitenberg and Schütz 1991 for a comprehensive review of this subject), the following conclusions can be drawn. Corticotectal neurons, which have long extending collaterals in cortical layer II/III and many more boutons, possibly activate

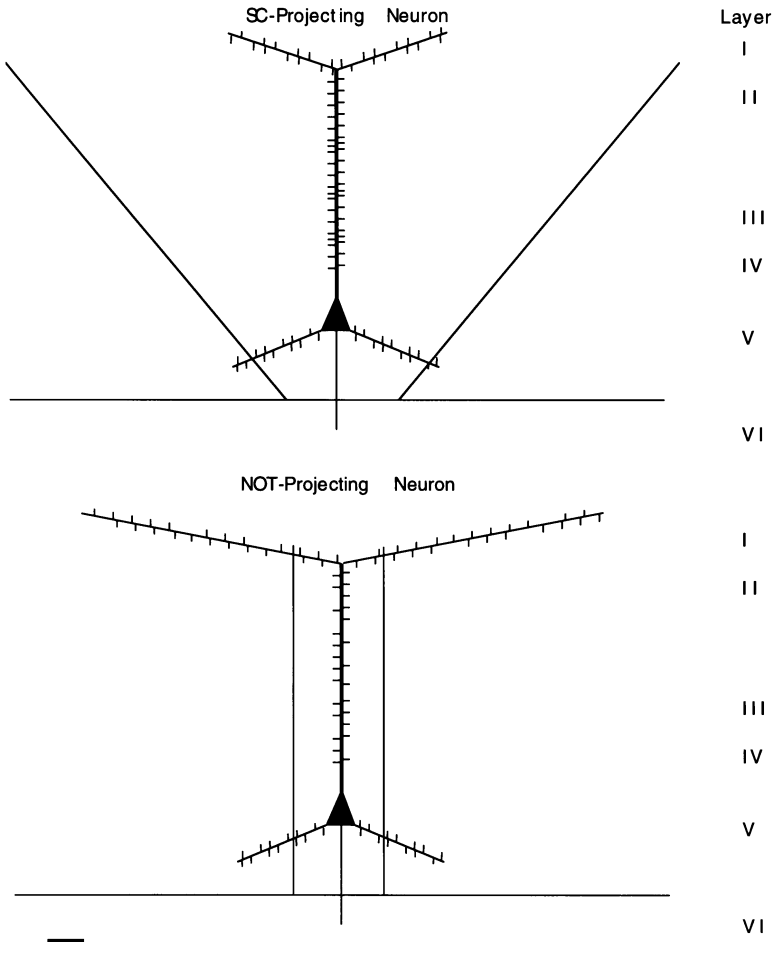

Fig. 11 Schematic representation of the special features of corticotectal and corticopretectal neurons. Note that differences between the two projection populations are present predominantly in layer *II/III*; no differences were seen in the parts of the neurons located in layers *V* and *VI*. *Scale bar* 100 µm

excitatory and inhibitory neuronal loops, thus providing a high spatial resolution for the information that will be transmitted to the SC. This information is needed by the SC for mediating accurate visual orienting responses. Because the visual cortex is retinotopically organized, the small lateral stimulation distance in slice preparation equals small distances in retinotopic coordinates and hence in visual space. EPSPs were most efficient if elicited at a position close to the recorded cell, namely at lateral distances up to 1000 µm. This value equals the distance of two neighboring corticotectal neurons with no overlap in their dendritic field. In contrast, corticopretectal neurons with ascending collaterals relatively close to their own apical dendrite therefore only activate other cortical neurons representing a similar spatial location and possibly the same preferred directions. Also, as indicated by the relatively low number of boutons on their axonal collaterals, they only activate few other neurons. Because of their far-reaching inputs in layer II/III, corticopretectal neurons should be capable of transmitting directional information of large parts of the visual field. Therefore, EPSPs have the steepest slope and highest efficiency if they are elicited from stimulation sites up to 1500 µm away from the recorded neuron, corresponding to a large part in the visual field. The directional information from large parts of the visual field is needed to support the globally organized optokinetic reflex mediated by the NOT.

In summary, both populations seem to be well suited, both in terms of their morphology and their intracortical connections, to transmit appropriate information to their subcortical targets. While corticotectal cells should be able to transmit information with good spatial resolution, subserving visual orienting, corticopretectal neurons should be capable of transmitting directional information from large parts of the visual field.

Acknowledgements We would like to thank H. Korbmacher for preparing excellent extracellular recording electrodes, I. Paas for her invaluable help with photos, and the Deutsche Forschungsgemeinschaft for supporting this work with grants KOGNET and Ey 8/17-2.

References

Agmon A, Conners BW (1992) Correlation between intrinsic firing patterns and thalamocortical synaptic responses of neurons in mouse barrel cortex. J Neurosci 12:319–329

Amitai Y (1994) Membrane potential oscillations underlying firing patterns in neocortical neurons. Neuroscience 63:151–161

Amitai Y, Friedman A, Conners BW, Gutnick MJ (1994) Regenerative activity in apical dendrites of pyramidal cells in neocortex. Cereb Cortex 3:26–38

Braitenberg V, Schütz A (1991) Anatomy of the cortex. Springer, Berlin Heidelberg New York

Burkhalter A (1989) Intrinsic connections of rat primary visual cortex: laminar organization of axonal projections. J Comp Neurol 279:171–186

Chagnac-Amitai Y, Luhmann H, Prince DA (1990) Burst generating and regular spiking layer 5 pyramidal neurons of rat neocortex have different morphological features. J Comp Neurol 296: 598–613

Chen W, Zhang JJ, Hu GY, Wu CP (1996a) Electrophysiological and morphological properties of pyramidal and nonpyramidal neurons in cat motor cortex in vitro. Neuroscience 73:39–55

Chen W, Zhang JJ, Hu GY, Wu CP (1996b) Different mechanisms underlying the repolarization of narrow and wide action potentials in pyramidal cells and interneurons of cat motor cortex. Neuroscience 73:57–68

Conners BW, Gutnick MJ (1990) Intrinsic firing patterns of diverse neocortical neurons. Trends Neurosci 13:99–104

Conners BW, Gutnick MJ, Prince DA (1982) Electrophysiological properties of neocortical neurons in vitro. J Neurophysiol 48: 1302–1320

Feldman ML, Peters A (1979) A technique for estimating total spine numbers on golgi-impregnated dendrites. J Comp Neurol 188: 527–542

Fellemann DJ, Van Essen DC (1991) Distributed hierarchical processing in the primary cerebral cortex. Cereb Cortex 1:1–47

Guthrie PB, Segal M, Kater SB (1991) Independent regulation of calcium by imaging dendritic spines. Nature 354:7–79

Hallman E, Schofield RB, Lin CS (1988) Dendritic morphology and axonal collateral of cortico-tectal, corticopontine and callosal neurons in layer 5 of the primary visual cortex of the hooded rat. J Comp Neurol 272:149–160

Harting JK, Updyke BV, Van Lieshout DP (1992) Cortico-tectal projections in the cat: anterograde transport studies of twenty-five cortical areas. J Comp Neurol 324:379–414

Hoffmann KP (1973) Conduction velocity in pathways from retina to superior colliculus in the cat: a correlation with receptive-field properties. J Neurophysiol 36:409–424

Hoffmann KP (1989) Functional organization of the optokinetic system of mammals. Prog Zool 37:261–271

Hoffmann KP, Distler C (1986) The role of direction selective cells in the nucleus of the optic tract of cat and monkey during optokinetic nystagmus. In: Keller EL, Zee DS (eds) Adaptive processes in the visual and occulomotor systems. Pergamon Press, Oxford, pp 261–266

Hoffmann KP, Schoppmann A (1975) Retinal input to direction selective cells in the nucleus tractus opticus of the cat. Brain Res 99:359–366

Hoffmann KP, Stone J (1985) Retinal input to the nucleus of the optic tract of the cat assessed by antidromic activation of ganglion cells. Exp Brain Res 59:395–403

Horikawa K, Armstrong WE (1988) A versatile means of intracellular labeling: injection of biocytin and its detection with avidin conjugates. J Neurosci Methods 25:1–11

Hübener M, Bolz J (1988) Morphology of identified projection neurons in layer 5 of rat visual cortex. Neurosci Lett 97:76–81

Hübener M, Schwarz C, Bolz J (1990) Morphological types of projection neurons in layers of cat visual cortex. Comp Neurol 301: 655–674

Huerta MF, Harting JK (1984) The mammalian superior colliculus: studies of its morphology and its connections. In: Venegas H (ed) Comparative neurology of the optic tectum. Plenum Press, New York, pp 687–773

Kasper EM, Larkman AU, Lübke J, Blakemore C (1994) Pyramidal neurons in layer 5 of rat visual cortex. I. Correlation among cell morphology, intrinsic electrophysiological properties and axon targets. J Comp Neurol 339:459–474

Katz B (1966) Nerve, muscle, and synapse. McGraw-Hill, New York

Katz LC, Burkhalter A, Dreyer WJ (1984) Fluorescent latex microspheres as a retrograde neuronal marker for in vivo and in vitro studies of visual cortex. Nature 310:498–500

Klein BG, Mooney RD, Fish SE, Rhoades RW (1986) The structural and functional characteristics of striate cortical neurons that innervate the superior colliculus and lateral posterior nucleus in hamster. Neuroscience 17:57–78

Koester SE, O'Leary DDM (1992) Functional classes of cortical projection neurons develop dendritic distinctions by class-specific sculpting of an early common pattern. J Neurosci 12: 1382–1393

Kuypers HGJM, Bentivoglio M, Catsman-Berrevoets CE, Bajros AT (1980) Double retrograde labeling through diverging axon collaterals, using two fluorescent tracers with same excitation wavelength, which labels different features of the cell. Exp Brain Res 40:383–392

Larkman AU (1991a) Dendritic morphology of pyramidal neurons of the visual cortex of the rat. I Branching patterns. J Comp Neurol 306:307–319

Larkman AU (1991b) Dendritic morphology of pyramidal neurons of the visual cortex of the rat. II. Parameter correlations. J Comp Neurol 306:320–331

Larkman AU (1991c) Dendritic morphology of pyramidal neurons of the visual cortex of the rat. III. Spine distributions. J Comp Neurol 306:332–343

Larkman AU, Mason A (1990) Correlations between morphology and electrophysiology of pyramidal neurons in slices of rat visual cortex. I. Establishment of cell classes. J Neurosci 10:1407–1414

Linden R, Perry VH (1983) Massive retinotectal projections in rat. Brain Res 272:145–149

Lohmann H (1994) Electrophysiological and morphological properties of corticocortical projection neurons in the visual cortex of the rat (abstract). In: Elsner N, Breer H (eds) Sensory Transduction. Thieme, Stuttgart, p 508

Lohmann H, Algür Y (1995) Spatio-temporal summation of synaptic activity in visual cortical pyramidal cells in vitro. Brain Res 671:275–281

Lohmann H, Rörig B (1994) Long range horizontal connections between supragranular pyramidal cells in extra striate visual cortex of the rat. J Comp Neurol 344:543–558

Mader W (1987) Axonale Arborisierung von physiologisch charakterisierten cortico-tectalen Zellen der Sehrinde der Katze. Doctoral thesis, University of Ulm

Mason A, Larkman A (1990) Correlations between morphology and electrophysiology of pyramidal neurons in slices of rat visual cortex. II. Electrophysiology. J Neurosci 10:1415–1428

McCormick DA, Conners BW, Lighthall JW, Prince DA (1985) Comparative electrophysiology of pyramidal and sparsely spined stellate neurons of the neocortex. J Neurophysiol 54: 782–806

Müller W, Connor JA (1991) Dendritic spines as individual compartements for synaptic Ca^{2+} responses. Nature 354:73–76

Nicoll A, Larkman A, Blakemore C (1993) Modulation of EPSP shape and efficacy by intrinsic membrane conductances in rat neocortical pyramidal neurons in vitro. J Physiol (Lond) 468: 693–710

Olavarria J, Montero VM (1989) Organization of visual cortex in the mouse revealed by correlating callosal and striate-extra striate connections. Vis Neurosci 3:59–69

Reitboeck (1983) Fiber microelectrodes for electrophysiological recordings. J Neurosci Methods 8:249–262

Rumberger A, Lohmann H, Hoffmann KP (1994) Electrophysiological and morphological comparison of cortico-tectal and cortico-pretectal neurons in rat visual cortex (abstract). In: Elsner N, Breer H (eds) Sensory transduction. Thieme, Stuttgart, p 509

Rumberger A, Lohmann H, Hoffmann KP (1995) Quantitative electrophysiological and morphological comparison of cortico-tectal and cortico-pretectal neurons in rat visual cortex (abstract). In: Elsner N, Menzel R (eds) Lernen und Gedächtnis. Thieme, Stuttgart, p 502

Schmidt M, Zhang HY, Hoffmann KP (1993) OKN-related neurons in the rat nucleus of the optic tract and dorsal terminal nucleus of the accessory optic system receive a direct cortical input. J Comp Neurol 330:147–157

Schofield RB, Hallman E, Lin CS (1987) Morphology of corticotectal cells in the primary visual cortex of hooded rats. J Comp Neurol 261:85–97

Schoppmann A, Hoffmann KP (1979) A comparison of visual responses in two pretectal nuclei and in the superior colliculus of the cat. Exp Brain Res 35:495–510

Sefton AJ, Mackay-Sim A, Baur LA, Cotte LJ (1981) Cortical projections to visual centers in the rat: an HRP study. Brain Res 215:1–13

Silva LR, Gutnick MJ, Connors BW (1991a) Laminar distribution of neuronal membrane properties in neocortex or normal and Reeler mouse. J Neurophysiol 66:2034–2040

Silva LR, Amitai Y, Connors BW (1991b) Intrinsic oscillations of neocortex generated by layer 5 pyramidal neurons. Science 251:432–435

Solomon JS, Doyle JF, Burkhalter A, Berbonne JM (1993) Different expression of hyperpolarization-activated currents reveals distinct classes of visual cortical projection neurons. J Neurosci 13:5082–5091

Tseng GF, Prince DA (1993) Heterogenity of rat corticospinal neurons. J Comp Neurol 335:92–108

Tseng GF, Parada I, Prince DA (1991) Double-labeling with rhodamine beads and biocytin: a technique for studying corticospinal and other projection neurons in vitro. J Neurosci Methods 31: 121–131

Wang Z, McCormick DA (1993) Control of firing mode of corticotectal and corticopontine layer 5 burst-generating neurons by norepinephrine, acetylcholine and 1S,3R-APCD. J Neurosci 13:2199–2216

Zhang HY, Hoffmann KP (1993) Retinal projections to the pretectum, accessory optic system and superior colliculus in pigmented and albino ferrets. Eur J Neurosci 5:486–500

Zilles K (1985) The cortex of the rat. A stereotaxic atlas. Springer, Berlin Heidelberg New York